

# Au-In-based Hermetic Sealing for MEMS Packaging for Down-Hole Application

VIVEK CHIDAMBARAM,<sup>1,3</sup> CHEN BANGTAO,<sup>1</sup> GAN CHEE LIP,<sup>2</sup>  
and DANIEL RHEE MIN WOO<sup>1</sup>

1.—Institute of Microelectronics, A\*STAR (Agency for Science, Technology and Research), 11 Science Park Road, Singapore Science Park II, Singapore 117685, Singapore. 2.—School of Materials Science and Engineering, Nanyang Technological University, Singapore, Singapore. 3.—e-mail: nachiappanvc@ime.a-star.edu.sg

Hermetic sealing of micro-electro mechanical systems (MEMS) sensors for down-hole application requires high-quality void-free bonds, with metallic hermetic sealing being widely used for this purpose. As most of the MEMS sensors cannot withstand high temperatures, transient liquid phase (TLP) bonding is promising for metallic sealing applications, since the re-melting temperature of the bond is much higher than the bonding temperature. In this paper, major issues involving TLP bonding, including non-uniform diffusion kinetics across the interface and the formation of intermetallic compounds prior to bonding for fast reactive metallic systems like Au-In, have been addressed by using diffusion barriers. The performance of various diffusion barriers that include Ti, Ni, and Pt has been evaluated. Ni has been determined to be a prospective candidate, since it averts diffusion to a certain extent prior to TLP bonding. The mechanical strength and hermeticity of the Au-In joints have also been characterized after aging at 300 °C up to 500 h. No major changes in the thermo-mechanical properties of the AuIn and AuIn<sub>2</sub> phases were observed and, hence, these phases are concluded to be thermally stable at this temperature regime. Improvements in hermeticity were confirmed when subjected to high-temperature thermal aging.

**Key words:** Transient liquid phase, intermetallic compounds, diffusion barrier, hermeticity, thermal aging, shear strength

## INTRODUCTION

Many industries are searching for electronics that can operate reliably in harsh environments, including extremely high temperatures. The oldest, and currently largest, user of high-temperature electronics is the down-hole oil and gas industry. In this application, the operating temperature is a function of the underground depth of the well. In the past, drilling operations have been carried out at temperatures of 150–175 °C, but declining reserves of easily accessible natural resources coupled with advances in technology have motivated the industry to drill deeper. However, the temperature in the

hostile wells can reach as high as 300 °C.<sup>1</sup> Micro-electro mechanical systems (MEMS) sensors are required for measurements during well drilling and for production management. During drilling, sensors used include temperature, pressure, radiation, acoustic, reactivity, and inclination.<sup>2</sup>

Sensor devices require the package to effectively isolate the chip physically from its environment by hermetic sealing of the package. The maintenance of hermeticity is critical for ensuring the reliable performance of MEMS devices. The hermetic seal prevents the atmosphere from leaking into the package and raising the pressure inside.<sup>3</sup> Thus, the existing approach is to use high-temperature intermetallic compounds (IMC) solder, i.e., through transient liquid phase (TLP) bonding. TLP bonding is a technique used to produce joints composed of

(Received August 7, 2013; accepted March 18, 2014;  
published online April 8, 2014)

IMCs at a low temperature, but ensures devices withstand higher temperatures during operations without failing.<sup>4,5</sup> Generally, the joints are made of metals, which have a low permeability and which can planarize over feed-throughs and other non-planarities. TLP bonding is attractive for MEMS packaging, since not all MEMS devices can withstand high bonding temperatures. The Au-In system has been chosen specifically for this investigation, since Au and In can inter-diffuse even at  $-50\text{ }^{\circ}\text{C}$ , and is believed to be the fastest among those of the transition metals. On the other hand, the re-melting temperature of Au-In TLP bonding ( $>454\text{ }^{\circ}\text{C}$ ) is higher than the conventionally used Au-Sn TLP bonding ( $>278\text{ }^{\circ}\text{C}$ ) and Cu-Sn TLP bonding ( $>415\text{ }^{\circ}\text{C}$ ). Moreover, from the processing point of view, In ( $156\text{ }^{\circ}\text{C}$ ) has a lower melting point than Sn ( $232\text{ }^{\circ}\text{C}$ ). Thus, the bonding temperature can be further reduced.<sup>6</sup> Furthermore, In-containing solder alloys are being preferred over the conventional Sn ones due to longer fatigue life, better mechanical properties, and reliability.<sup>7</sup>

Wafer-to-wafer bonding is gaining momentum in the large volume MEMS foundries due to its higher yield.<sup>2,8</sup> However, wafer level bonding (WLB) is limited by the temperature ramp rate, when compared to chip level bonding. Very high ramp rates are required to avert the transformation of the low melting interlayer into IMCs, prior to the melting point of the interlayer for some of the fast reactive metallic systems like Au-In or Cu-In. Better bond quality could be achieved for fast reactive metallic systems by using very high ramp rates. However, such ramp rates are not feasible for WLB due to the larger surface area of the samples. In this work, the performance of different nano-scale thin film diffusion barriers for achieving void-free hermetic joints in wafer level bonding has been studied. The reliability of the Au-In joints in rugged environments has been characterized at  $300\text{ }^{\circ}\text{C}$  for 500 h in order to fulfill the minimum requirement for down-hole applications, which is typically 2 weeks.<sup>9,10</sup>

### DESIGN OF AU-IN TLP BONDS

Several factors need to be considered, when designing a fluxless TLP bond. The material system, the thickness of the interlayer metal, and the heating rate will determine the final quality of the bond.<sup>6</sup> Two different compositions were evaluated in this work. The first composition has a higher concentration of Au in the bond with an In mole-fraction of 0.45, in order to achieve multiple Au-In phases. The respective Au and In film thickness chosen for this purpose are 1 and  $1.26\text{ }\mu\text{m}$ . The second composition is proportioned to form an  $\text{AuIn}_2$  compound throughout the bond. The respective Au and In film thicknesses selected for this purpose are 0.6 and  $1.8\text{ }\mu\text{m}$ . For the purpose of adhesion of these metallic thin films on  $\text{SiO}_2$ , the Au and/or In thin

films were always deposited on Ti and Pt thin films of thicknesses of 0.2 and  $0.05\text{ }\mu\text{m}$ , respectively.

A TLP bond is formed by stacking the low melting interlayer In over the parent metal Au. The Au-In TLP proceeds through 4 stages during the formation process. In the first stage, the parent metal Au and the low melting interlayer In are placed into contact and the multi-stacked thin films are heated to melt the In. In the second stage, the molten In interlayer flows over and seals the wafer topography, such as lateral feed-throughs. During this stage, the molten interlayer rapidly reacts with the parent metal to form high melting IMCs. In stage 3, the joint undergoes isothermal solidification as the last of the liquid In interlayer is transformed into IMCs. After the transformation of the interlayer, the melting temperature of the joint is raised from the melting point of the interlayer ( $156\text{ }^{\circ}\text{C}$ ) to the melting point of the IMC, which is either AuIn phase ( $509\text{ }^{\circ}\text{C}$ ) or  $\text{AuIn}_2$  phase ( $540.7\text{ }^{\circ}\text{C}$ ) or a mixture of both.<sup>4</sup>

Au-In bonding was performed with and without the diffusion barriers. The effect of stacking a protective Au coverage layer over the In interlayer on the bond quality was also studied. The purpose of stacking Au thin film over In is to protect the latter from oxidation, prior to the TLP bonding. The thickness of the protective coverage layer used in this study is  $0.03\text{ }\mu\text{m}$ . The inter-diffusion between Au and In can occur even at  $-50\text{ }^{\circ}\text{C}$ , and is believed to be the fastest among those of the transition metals.<sup>11</sup> Hence, the impacts of three metallic diffusion barriers, namely Ti, Pt, and Ni, on the Au-In diffusion kinetics were evaluated. The diffusion barrier is sandwiched between the parent metal Au and the low melting In interlayer. Various diffusion barrier thicknesses ranging from 10 to  $30\text{ }\mu\text{m}$  were evaluated and the optimized thickness was determined to be  $20\text{ }\mu\text{m}$ . Four kinds of material stacking schemes were evaluated in this work and are illustrated in Fig. 1.

### EXPERIMENTAL PROCEDURES

Eight-inch (c.20-cm) wafers were used for Au-In TLP bonding and the width of the sealing ring used for this investigation is  $100\text{ }\mu\text{m}$ . Au/In inter-diffusion was evaluated on Si substrates with  $0.5\text{-}\mu\text{m}$ -thick  $\text{SiO}_2$ , in order to isolate the metallic layers from the substrate. The patterning of the sealing ring was done by lithography, using a  $7\text{-}\mu\text{m}$  MAN 1440 (Micro-resist Technology, Berlin, Germany) negative photoresist as masking material. Au/In thin films with and without diffusion barriers were deposited using a VES 2550 E-beam evaporator (Temescal, Livermore, CA, USA) sequentially, without breaking the vacuum. The deposition temperature never exceeded  $40\text{ }^{\circ}\text{C}$  and the deposition rate never exceeded  $\sim 5\text{ }\text{\AA}/\text{s}$  for any of the metals. Film thickness was monitored with a quartz-crystal oscillator during evaporation. The sealing ring was

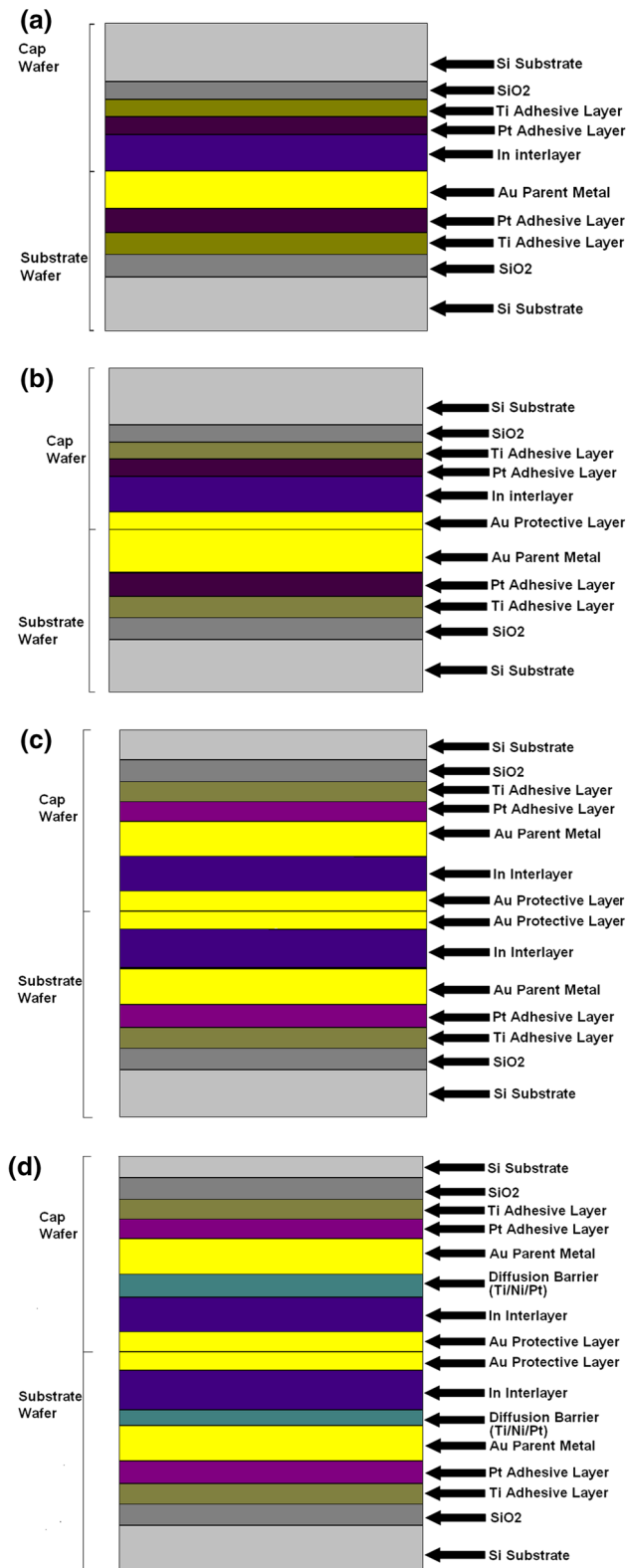


Fig. 1. Material stack of TLP samples emulating actual Au-In TLP bonding. (a) Without Au protective coverage layer, (b) with Au protective coverage layer, (c) without diffusion barrier, and (d) with Ti/Ni/Pt diffusion barrier. Au and In thicknesses vary by samples to create the mentioned two different material ratios.

patterned by the lift-off process, using REM 660 negative resist stripper (Micro-resist Technology).

Chip level bondings were performed using a flip-chip (FC) 150 bonder (Smart Equipment Technology, Saint Jeoire, France). All the chip level bondings were executed without using any diffusion barriers and the size of the individual chip was 16 mm × 16 mm. The bonding temperature was fixed at 200 °C and the bonding time and the bonding pressure were optimized accordingly. The impact of ramp rates on the bond quality was assessed, by using different ramp rates that include 50, 75, and 100 °C/min. Wafer-level Au-In TLP bonding was conducted in a vacuum environment using an EVG 520 wafer level bonder (EV Group, St. Florian am Inn, Austria).

WLB with and without diffusion barriers were executed at a fixed ramp rate of 30 °C/min. Higher ramp rates could not be achieved using this existing wafer level bonder for the eight-inch wafer. The bonding conditions were optimized with the sole objective of attaining void-free hermetic joints. The bonding quality was evaluated at 200 °C for various times that include 15, 30, and 45 min. The bonding pressure was varied between 5 and 10 MPa for wafers without diffusion barriers and between 5 and 15 MPa for wafers with diffusion barriers.

Qualitative assessment of the bond was performed using a Sonix HS 3000 C-SAM (Sonix, Springfield, VA, USA) with a 230-MHz transducer with a spatial resolution of 10–20 μm. Different locations on the bonded wafer were chosen for these analysis in order to confirm the consistency of the bonding quality. However, the C-SAM is limited to a specific location. Hence, through-scan mode was also used in order to infer the overall bonding quality. The bonded wafers were subsequently diced into 16 mm × 16 mm dies, using dicing saw equipment at a dicing speed of 5 mm/s. Quantitative assessment of the bond was performed using helium leak rate testing according to MIL-STD-883. The bonded chip was placed in a high helium pressure bombing chamber for 4 h, following which, the samples were transferred to the helium spectrometer to monitor the leakage of He.

The bonded dies were subjected to thermal aging at 300 °C for 100, 300, and 500 h. The samples subjected to different bonding and aging conditions were mounted and cross-sectioned for scanning electron microscopy (SEM) (JEOL 7600; JEOL, Tokyo, Japan). Energy-dispersive spectroscopy (EDX) analysis was used to study the compositions of the reaction zone. The bonded dies were also subjected to a thermal cycling environment from –65 to 150 °C for 500 cycles, in order to study the impact of thermo-mechanical stresses on the bond quality. The mechanical properties of the bonded joint for various bonding and aging conditions were evaluated using die shear tests. Ten samples were

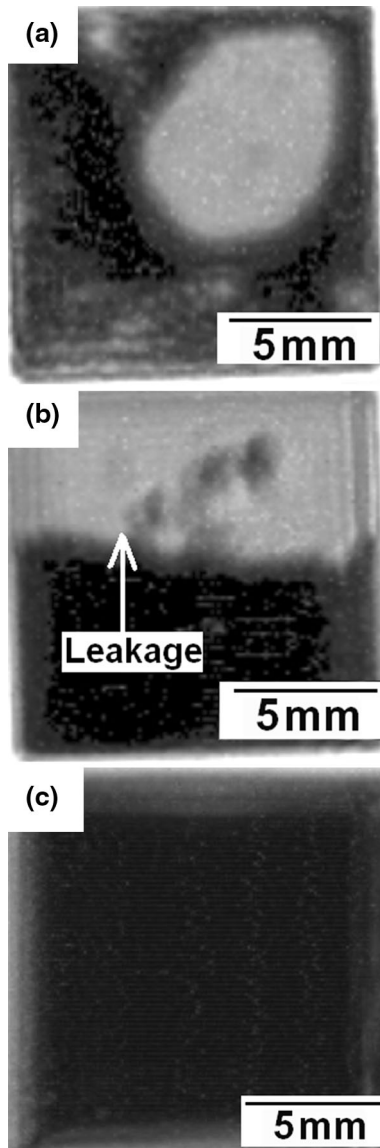


Fig. 2. Through-scan images of chip level bonded dies subjected to different ramp rates (a) 50 °C/min, (b) 75 °C/min, and (c) 100 °C/min.

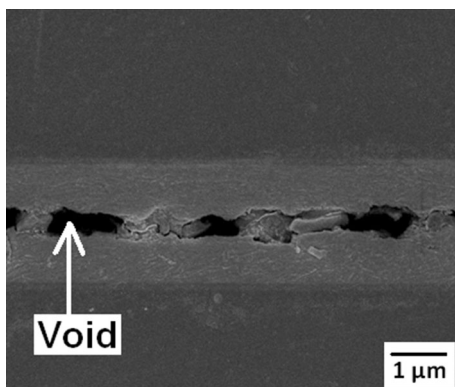


Fig. 3. SEM cross-section of Au/In wafer level bonding without diffusion barriers.

evaluated for each bonding, aging and thermal cycling conditions. The shear test was conducted with a Dage 4000 shear tester (Nordson Dage, Aylesbury, Bucks, UK), employing a load cell capable of recording forces up to 100 kg. High-temperature mechanical testing of the joint was performed by hot shear testing at 250 °C. Again, 10 samples were evaluated for each bonding, aging, and thermal cycling conditions.

### IMPACT OF RAMP RATE ON THE BOND QUALITY

It was determined that the temperature ramp rate has a direct impact on the Au-In bond quality. Die level bonding was performed on Au-In TLP samples with and without Au protective coverage layer (Fig. 1a, b). Higher bonding pressure was required to achieve better bond quality for Au-In TLP samples without the Au protective coverage layer. This requirement for higher bonding pressure could be attributed to the necessity of cracking indium oxides formed at the interface. Through-scan analysis was used for preliminary screening of the bonds. In through-scan images, the dark region represents air while the white region represents water. The leakage of water observed in the through-scan analysis of chip level bonded dies confirms the lack of hermeticity of the bonds, when a slower ramp rate was used (Fig. 2a). Improvement in hermeticity was observed with the increase in the ramp rate (Fig. 2b), where no leakage of water was observed, when a ramp rate of 100 °C/min was used (Fig. 2c). Very high ramp rates are required to avert the transformation of the low-melting interlayer like In into IMCs prior to bonding. The formation of these IMCs prior to bonding due to slower ramp rates results in the generation of voids (Fig. 3). This is because these IMCs will not melt during the actual bonding temperature, as their re-melting temperature is much higher than the TLP bonding temperature.

The inter-diffusion between Au and In can occur even at -50 °C, and it is believed to be the fastest among those of the transition metals.<sup>11</sup> Good bond quality at die level could be achieved for such fast reactive metallic systems by using very high ramp rates together with isolating the low melting interlayer In and the parent metal Au, prior to bonding. However, such high ramp rates are not feasible for WLB and only possible for chip level bonding. The state-of-the-art wafer level bonder can achieve a maximum ramp rate of 45 °C/min.

### LIMITATIONS IN RAMP RATE IN WAFER LEVEL BONDER

There are several limitations in the commercial wafer bonder with respect to the temperature ramp rate. The thermal time constant of the system determines the maximum heating and cooling rates



that can be achieved. Generally, the configuration of the existing commercial wafer-level bonder produces a large thermal constant for several reasons. First, the fixture's bottom and top sandwich plates need to be heated along with the wafers. This is a much larger mass by several orders of magnitude as compared to the wafers themselves. More thermal mass means that more heat needs to be moved into the system or removed in order to change the temperature. Second, getting the heat in and out of the system is a challenge, especially when the bond chamber is pumped down to a low vacuum atmosphere. This is because the system relies on thermal conduction across long distances in order to heat the fixtures and wafers. Moreover, the heaters used to generate the heat are not placed right next to the wafer stack. They are placed well below the sandwich plates in the heater assemblies. The heat has to travel through all of the materials between the heaters and the wafers to cause any temperature rise in the wafers. Any additional thermal resistance in the heating will lead to a larger thermal time constant and, therefore, longer heating times are required for WLB.

#### WAFER LEVEL BONDING WITHOUT DIFFUSION BARRIER

No bond could be achieved between the cap and the substrate wafers, when Au and In layers were stacked over one another (Fig. 1c). This could be attributed to the formation of IMCs prior to the bonding. However, a bond could be achieved when the Au and In layers were isolated and brought into contact just prior to the melting point of the interlayer (Fig. 1a). In this case, Au and In were deposited on the substrate and cap wafers, respectively, they were brought into contact only when both the substrate and the cap wafers were at 150 °C. However, the quality of the bonding was poor due to the presence of native indium oxides inhibiting TLP bonding despite using a high bonding pressure of 10 MPa. No bonding could be achieved when a low bonding pressure of 5 MPa was used. However, bonding quality dramatically improved when the In layer on the cap wafer was covered by a protective Au layer of 0.03  $\mu\text{m}$  thickness (Fig. 1b). Bonding could be achieved with a low bonding pressure of 5 MPa in such cases. However, bonding quality could still be significantly improved by increasing the bonding pressure to 10 MPa. This was confirmed by through-scan analysis, as illustrated in Fig. 4. A similar trend was observed for both the compositions. However, the yield of hermetically sealed dies was higher for the composition with the higher In mole-fraction.

Optimization of the bonding parameters was carried out with the objective of ensuring void-free bonds. The bonding pressure has a direct impact on solder splashing, which is critical in determining the adaptability of the Au-In TLP bonding to test

vehicle with populated MEMS devices. C-SAM analysis was used to confirm the presence of solder splashing, since this technique allows focusing on individual bonded dies. Solder splashing was observed on Au-In bonded dies, which were subjected to a bonding pressure of 15 MPa (Fig. 5). On the other hand, no solder splashing was observed on Au-In bonded dies bonded at 10 MPa.

It was determined that 100% yield could not be achieved even for higher bonding pressures, despite using an Au protective coverage layer. There was a considerable number of dies in an eight-inch wafer, which were not hermetically sealed. Multi-stacking of Au/In on both the substrate and the cap wafers was also evaluated (Fig. 1c). Bonding could not be achieved despite using a protective Au coverage layer and a higher bonding force. Even bonding pairs subjected to 15 MPa delaminated during through-scan analysis for the mentioned reasons.

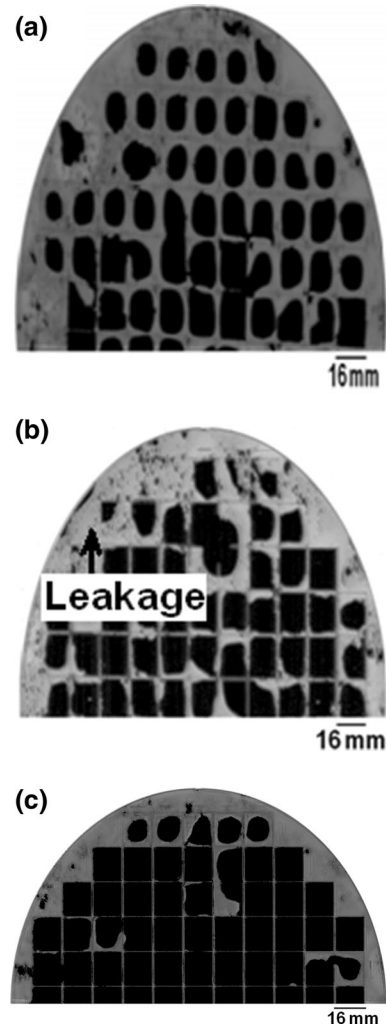


Fig. 4. Through-scan images of composition with higher In mole-fraction (a) without protective Au coverage layer using a bonding pressure of 10 MPa, (b) with protective Au coverage layer using a bonding pressure of 5 MPa, or (c) 10 MPa.

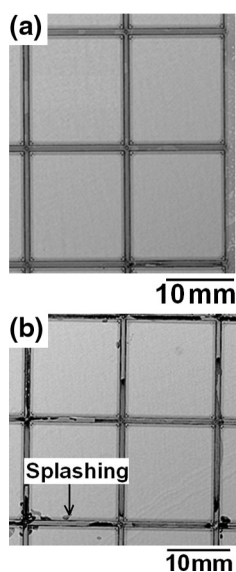


Fig. 5. Impact of bonding pressure on solder splashing, wafers bonded at (a) 10 MPa and (b) 15 MPa.

### WAFER LEVEL BONDING WITH DIFFUSION BARRIER

WLB was further performed by using diffusion barriers between the low melting In interlayer and the parent metal Au. Similar multi-layer thickness was used for both the substrate and the cap wafers. The performance of three conventional diffusion barriers, i.e., Ti, Ni, and Pt, was evaluated for Au/In multi-stacked wafers (Fig. 1d). The composition with the higher mole-fraction of In (0.67), which is designed to form  $\text{AuIn}_2$  phase throughout the bond was selected for this investigation against the composition with the lower In mole-fraction (0.45), which results in a mixture of AuIn and  $\text{AuIn}_2$  phases. This is because slightly higher content of In would help to reduce the cracks at the interface.

Bulk diffusion is believed to be dominant at higher temperatures that can create a liquid/solid interface, while solid-state diffusion at low temperatures might be controlled by grain boundary diffusion. Bjontegaard et al.<sup>12</sup> has reported an activation energy of only 0.23 eV for the diffusion-controlled growth of Au-In solid-state reaction, suggesting the formation of IMCs is imminent even at room temperature. The thickness of the diffusion barrier investigated in this work was 10, 20, and 30 nm. An additional advantage of using a diffusion barrier is that the volume of the low melting interlayer In could be substantially reduced. Void-free and crack-free joints could be achieved with an In interlayer thickness of  $<4 \mu\text{m}$ , with all the In interlayer transformed into IMCs after bonding. A large amount of liquid In is otherwise required for conventional TLP bonding without diffusion barriers in order to form a continuous layer of IMCs; in particular, to create a liquid/solid interface between the interlayer and the parent metal.

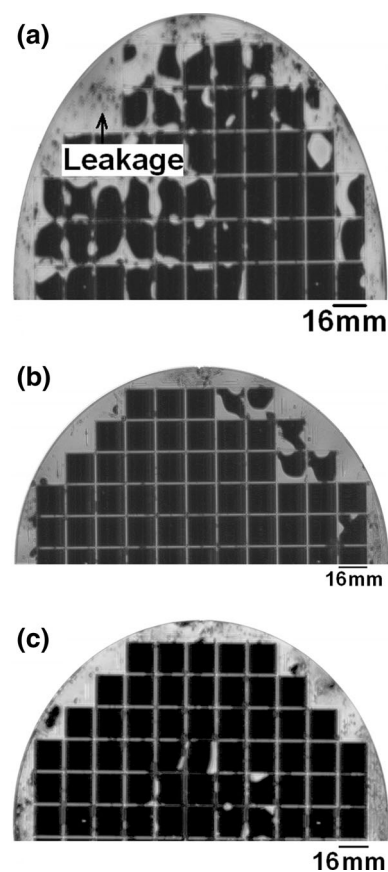


Fig. 6. Through-scan images of Au/In multi-stacked wafers using (a) Ti, (b) Pt, (c) Ni diffusion barriers.

The introduction of a thin 10-nm-thick Ti diffusion barrier did not have any improvement in the bonding quality, although Zhang et al.<sup>11</sup> has reported that the introduction of a thin Ti barrier (10 nm) can effectively slow down interdiffusion at room temperature. Even increasing the barrier thickness to 30 nm did not result in any improvement of the bonding quality, indicating that the Ti barrier does not inhibit the formation of Au-In IMCs during the temperature ramp-ups (Fig. 6). No difference in the interface composition was observed in samples with and without a Ti diffusion barrier between the Au-In thin films. The interface was only composed of  $\text{AuIn}_2$  IMC. However, the presence of Ti could not be traced due to the SEM-EDX limitations.

Better bond quality was achieved when using Pt or Ni diffusion barriers as illustrated in Fig. 6, indicating that the Pt and Ni diffusion barriers could better mitigate the Au-In rapid interdiffusion. This could be attributed to the presence of an Au-rich phase with limited solubility of In at the interface. SEM-EDX analysis suggests that this phase could be  $\alpha_1$  phase for Au-In TLP samples with Ni diffusion barrier and (Au) solid solution phase for Au-In TLP samples with Pt diffusion barrier.<sup>13,14</sup> The inter-diffusion of Au and In in these Au-rich

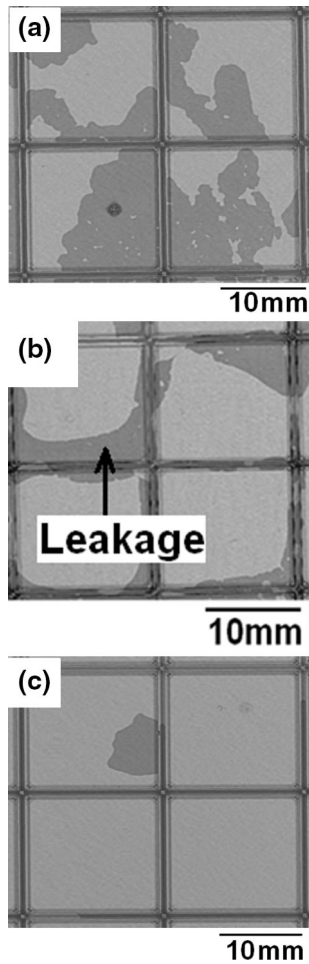


Fig. 7. C-SAM images of selective dies with leakage from bonded wafers with different diffusion barriers: (a) Ti, (b) Pt, (c) Ni.

phases are lower than the inter-diffusion co-efficient Au and In in AuIn or AuIn<sub>2</sub> phases.

The yield of hermetically sealed dies in an eight-inch wafer was higher for the Ni thin film barrier as compared to Pt. This suggests that Ni serves as a better diffusion barrier. This could be attributed to the volume-fraction and the inter-diffusion co-efficient parameters of the  $\alpha_1$  phase. However, seepage of water was observed in a few dies even for bonded pairs involving Ni diffusion barrier. This was confirmed by both through-scan analysis and C-SAM analysis. C-SAM analysis was performed on selected leaked dies involving all the three diffusion barriers to determine the magnitude of leakage, as illustrated in Fig. 7. In C-SAM images, the gray areas represent water and the white areas represent air. Thus, the C-SAM images confirmed that the magnitude of leakage is the least for Ni diffusion barrier, followed by the Pt diffusion barrier.

Optimized diffusion barrier thickness was determined to be 20 nm. Furthermore, thicker diffusion barrier will hamper the TLP bonding process. A slightly higher bonding force is required for WLB with diffusion barriers, when compared to WLB

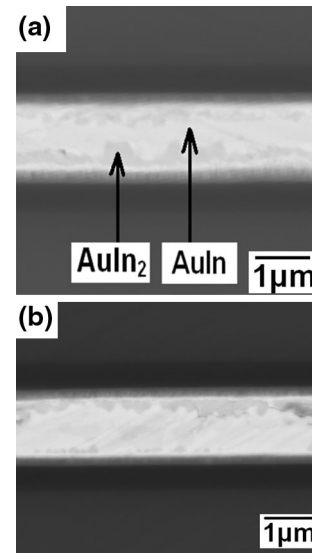


Fig. 8. SEM-BSE images of dies with less In mole-fraction (a) before thermal aging and (b) after thermal aging at 300 °C for 500 h.

without diffusion barriers. The optimized bonding conditions at 200 °C for AuIn TLP bonding with Ni diffusion barrier were 30 min (bonding time) and 15 MPa (bonding pressure). However, 100 % yield could still not be achieved for Au-In TLP-bonded wafer with Ni diffusion barrier.

### MICROSTRUCTURE CHARACTERIZATION

Between the two compositions investigated in this work, it was determined that the composition with the lower In mole-fraction resulted in a microstructure comprising the AuIn and AuIn<sub>2</sub> phases. The second composition with the higher In mole-fraction resulted eventually in an AuIn<sub>2</sub> phase throughout the bond.  $\alpha_1$  phase was observed in the Au-In samples with Ni diffusion barrier after TLP bonding. Au solid solution phase was observed in Au-In samples with the Pt diffusion barrier. The size difference between Au and In is well within the 15 % criterion of Hume Rothery. Moreover, Au and Pt are neighbors in the periodic system.<sup>15</sup> However, the Au-rich phases could not be detected in the aged samples for the In-rich compositions. Based on these findings, it could be interpreted that Au-rich phases are metastable for this particular composition and the mentioned TLP bonding conditions.  $\alpha_1$  has been reported to be very stable by Waelti et al.<sup>16</sup> in the Ni/In/Au system after annealing at 160 °C for 1,000 h. However, the composition and the isothermal solidification conditions are different.

Thermal aging at 300 °C for 500 h resulted in no major changes in the morphology for the lower In mole-fraction samples (Fig. 8), where the Au metallization and In interlayer were isolated, prior to bonding. This could be credited to the high melting temperature of these IMCs. Back-scattered electron imaging (BSE) mode was used for the microstructure

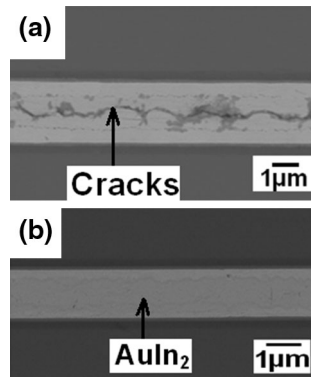


Fig. 9. SEM-BSE images of multi-stacked Au/In dies involving diffusion barriers with varying In mole-fraction (a) 0.45 and (b) 0.67. Au-rich phase was not observed at the interface for aged samples.

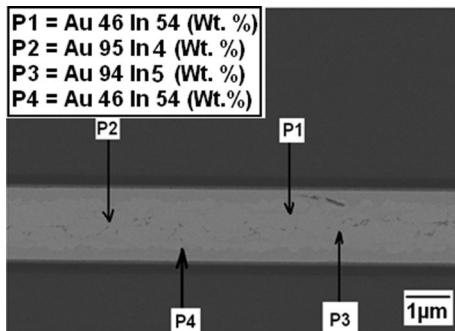


Fig. 10. Cross-section SEM and EDX analysis for AuIn samples with Pt diffusion barrier after TLP bonding.

characterization, since AuIn and the AuIn<sub>2</sub> phases could not be distinguished using secondary electron imaging (SEI) mode of the SEM. Although AuIn<sub>2</sub> and AuIn phases are present in the samples before and after thermal aging at 300 °C for 500 h, the volume-fraction varied. No specific trend was observed. In addition to the bond quality, the difference in the volume-fraction of these two phases could also account for the variation in the shear and hot shear strength results. It was also confirmed that all the In interlayer was consumed to form IMCs and no free In interlayer existed in the bonds.

For Au/In multi-stacked wafers, a better hermetically sealed joint could be easily achieved with the higher In mole-fraction. Cracks were observed at the interface for compositions with lower In mole-fraction, as illustrated in Fig. 9. This is because a large amount of liquid In is required in order to create a liquid/solid interface between the interlayer and the parent metal. Moreover, a large amount of liquid interlayer ensures good wetting of the metallization. Furthermore, volume shrinkage during IMC formation and isothermal solidification is observed to be higher for compositions with lower In mole-fraction. Composition with lower In mole-fraction (0.45) resulted in a microstructure comprising of

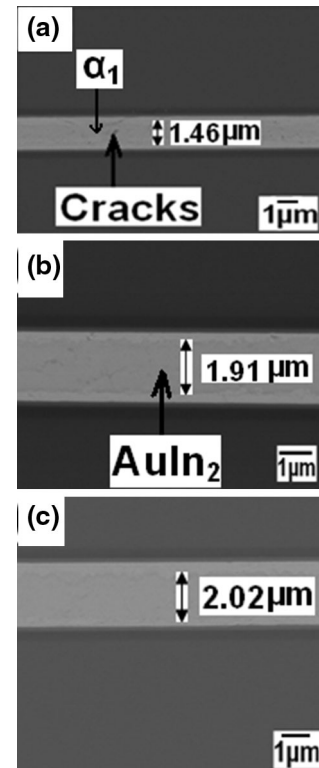


Fig. 11. SEM-BSE images of multi-stacked Au/In dies involving Ni diffusion barrier before and after thermal aging (a) without thermal aging, (b) aged at 300 °C for 300 h, and (c) 500 h.

both AuIn and AuIn<sub>2</sub> IMCs, while the microstructure of the samples with higher In mole-fraction (0.67) comprised of only AuIn<sub>2</sub> IMC. Macro-cracks were observed only in the reaction zone with both AuIn and AuIn<sub>2</sub> IMCs, while micro-cracks were observed in the reaction zone with only AuIn<sub>2</sub> IMC. Based on these observations, it can be concluded that the volume shrinkage of AuIn IMC from liquid is higher than AuIn<sub>2</sub> IMC.

The presence of diffusion barriers could not be traced by SEM-EDX analysis due to their nano-scale thicknesses. Better quality joints, i.e., bonds with minimal voids/micro cracks were observed for Au-In multi-stacked dies involving Pt and Ni diffusion barriers. This could be primarily attributed to the presence of Au-rich phases close to the interface, for the mentioned reasons. The In content in  $\alpha_1$  phase was roughly around 8 wt.% for Au-In samples with Ni diffusion barrier, while the In content in (Au) phase for Au-In TLP samples with Pt diffusion barrier was lower, roughly in the range of 4–5 wt.% (Fig. 10). Thus, it could be concluded that the isothermal solidification is influenced by the presence of diffusion barrier metals. However, introduction of these diffusion barriers between the Au and In thin films did not lead to a major impact in terms of volume shrinkage during IMC formation and isothermal solidification.

It should be noted that the thickness of intermetallics increases with time, indicating that the



phase evolution continues during thermal aging. No  $\alpha_1$  or (Au) phases were detected in the aged samples. The intermetallic was primarily composed of AuIn<sub>2</sub>. The volume-fraction of voids/micro cracks was slightly lower for Au/In multi-stacked dies involving Ni diffusion barrier, when compared to other TLP samples. The pace of growth was faster during the initial phase of thermal aging at 300 °C. The IMCs of the samples aged for 500 h were only slightly thicker than the ones aged for 300 h (Fig. 11). Thus, the growth of IMCs during thermal aging at 300 °C was confirmed. In addition to the growth of IMCs, minimization of micro-cracks/voids was observed during thermal aging at 300 °C. Better bond quality was achieved for Au/In multi-stacked wafers with Ni diffusion barrier, which were subjected to thermal aging at 300 °C compared to the ones that were not thermally aged. The quality of the bonds using Ni diffusion barrier improved during thermal aging at 300 °C. It was once again confirmed that no unreacted In interlayer existed in the joint despite using diffusion barrier.

### JOINT STRENGTH CHARACTERIZATION

In order to determine the strength of the joints, shear tests were performed on bonded samples before and after thermal annealing. Die-shear testing was performed according to MIL-STD-883G. The die shear strength is defined as the maximum force required to break the attach bond. Shear strength is one of the most important parameters for bond quality evaluation. High bond strength is always required for the package structure, since mechanical support is one of the basic functions of the package. It is expected that the mechanical shear strength will depend greatly on various aspects of the bond quality, including microstructure changes and the formation of IMCs during both bonding and subsequent thermal aging.<sup>2,17,18</sup>

In addition to room temperature shear testing, hot shear testing at 250 °C was also performed. It was not possible to perform hot shear testing at 300 °C due to strain gauge limitations. The hot shear testing assumes more significance as it confirms the absence of low melting interlayer like In, which has a melting point of 156 °C. The shear

strength result of those samples, where the failure was not at the interface, has not been included.

Shear strength as well as hot shear strength at 250 °C for composition with less In mole-fraction (0.45) is listed in Table I. The shear strength results were aligned with the microstructure characterization and C-SAM analysis. Shear strength and hot shear strength were the smallest for samples without the Au protective coverage layer. Although the substrate wafers with the Au metallization and the cap wafers with In interlayer were brought into contact only prior to bonding (Fig. 1a), many bonded dies delaminated during thermal aging at 300 °C for various durations ranging from 100 to 500 h. This can be attributed to the presence of indium oxide (In<sub>2</sub>O<sub>3</sub>), which hampers the TLP bonding process and, thereby, resulted in the formation of voids. This phenomenon is consistent despite using higher bonding pressure for cracking intermediate indium oxides. No major difference between the shear strength and hot shear strength results were observed. This could be attributed to the pervasive presence of voids at the interface.

Higher room-temperature shear strength and hot shear strength results were obtained for samples with a thin protective Au coverage layer over the In interlayer on the cap wafer (Fig. 1b). There was no delamination of bonded dies during thermal aging at 300 °C. There was a significant improvement in terms of bond quality by using the protective Au coverage layer, since the formation of indium oxides at the interface has been averted. The slight variation between the room-temperature shear and hot shear strength results could be attributed to the phase transformation between the AuIn and AuIn<sub>2</sub> phases and also the volume-fraction of these two phases. However, all the dies were not hermetically sealed in Au-In wafer level bonding despite using the Au protective coverage layer over In and bringing them into contact only prior to bonding, i.e., at 150 °C. The shear and hot shear strength of these dies were very low. However, the presence of these dies has been greatly reduced by using a thin protective coverage layer.

The shear strength of Au/In multi-stacked wafers involving different diffusion barriers for the composition with higher mole-fraction of In (0.67) are

**Table I. Impact of a thin protective Au coverage layer on shear and hot shear strength results**

S. no.	Without Au protective coverage layer		With Au protective coverage layer	
	Shear strength (MPa)	Hot shear strength (MPa)	Shear strength (MPa)	Hot shear strength (MPa)
1.	7.82	3.38	55.02	59.79
2.	10.03	9.65	41.46	45.32
3.	8.48	19.13	33.85	38.51
4.	18.42	16.91	27.47	25.44
5.	2.37	5.67	52.15	30.26

**Table II. Performance evaluation of different diffusion barriers**

S. no.	Ti diffusion barrier			Pt diffusion barrier			Ni diffusion barrier		
	Before aging (MPa)	After aging (MPa)		Before aging (MPa)	After aging (MPa)		Before aging (MPa)	After aging (MPa)	
		300 h	500 h		300 h	500 h		300 h	500 h
1.	15.11	22.63	28.42	49.27	40.48	54.62	62.17	71.42	78.37
2.	13.84	18.58	25.73	63.04	43.5	46.75	55.75	76.34	74.25
3.	20.93	5.41	7.28	36.72	55.69	50.73	57.88	70.21	63.04
4.	11.73	15.72	9.42	30.61	48.16	57.42	41.02	64.36	69.41
5.	6.62	25.19	29.63	38.93	33.81	38.54	45.9	60.7	75.98

listed in Table II. Very low shear strength was observed for samples with a Ti diffusion barrier before and after thermal aging at 300 °C for various durations. This confirmed the fact that Ti does not serve as a good diffusion barrier for Au/In multi-stacked wafers during wafer-level bonding. No major difference in shear strength was observed in the aged samples involving a Ti diffusion barrier. Higher shear strength was observed for samples involving a Pt diffusion barrier. This could probably be attributed to the presence of (Au) phase at the interface resulting in partial mitigation of the inter-diffusion of Au and In, prior to bonding. A general trend of increase in shear strength was observed for the aged samples involving a Pt diffusion barrier. This could be attributed to the growth of AuIn<sub>2</sub> IMCs during thermal aging at 300 °C.

Highest shear strength was observed for Au/In multi-stacked wafers using Ni diffusion barrier. This, indicates that Ni serves as a better diffusion barrier. This could be attributed to the reduced inter-diffusion between Au and In in the  $\alpha_1$  phase. Similar increase in shear strength was observed during thermal aging, which could be attributed to the growth of AuIn<sub>2</sub> IMCs (Fig. 11). No major difference in the shear and hot shear strength values were observed for Au/In multi-stacked wafers with a Pt or Ni diffusion barrier. This could be attributed to the fact that AuIn<sub>2</sub> is a high melting IMC with a melting temperature of 495 °C. Thus, the aging temperature of 300 °C, which represents the homologous temperature of only 0.6, did not have a tangible impact on the thermal stability of the AuIn<sub>2</sub> phase. No major degradation in the shear and hot shear strength results were observed for samples involving AuIn<sub>2</sub>, which were subjected to thermal cycling from -65 to +150 °C for 500 cycles, despite being reported as a brittle phase. Moreover, AuIn<sub>2</sub>, is reported to be less brittle than Cu<sub>3</sub>Sn and Cu<sub>6</sub>Sn<sub>5</sub>, based on nano-indentation results, indicating that the chances of AuIn<sub>2</sub> serving as a crack nucleation site is very small.<sup>11</sup>

Delamination of bonded joints was observed during thermal aging of dies with a Ti diffusion barrier at 300 °C for durations ranging up to 500 h. However, no delamination was observed for the same

aging conditions for dies at the same aging conditions with Pt or Ni diffusion barriers. A few dies with Pt and Ni diffusion barriers also possessed lower shear/hot shear strengths. However, the presence of such dies in an eight-inch wafer involving numerous dies is less. The maximum yield of dies with higher shear/hot shear strengths was achieved with a Ni diffusion barrier.

### HERMETICITY CHARACTERIZATION

C-SAM and through-scan analysis can be used only for qualitative hermeticity characterization. Hence, helium leak rate testing was used for quantitative hermeticity characterization. The primary reasons for choosing a large test vehicle involving 16 × 16 mm<sup>2</sup> is to accommodate the fine helium leak rate testing requirements. Furthermore, a 100- $\mu$ m cavity was etched by Si deep reactive ion etching technique (DRIE) by using STS ICP DRIE equipment, since fine leak helium leak rate testing results are valid only for packages with a minimum volume of 0.05 cm<sup>3</sup>. The hermeticity of the bond quality was qualified using the MIL-STD-883 for fine helium leak rate testing. The fine He leak check consists of pressurizing the sample with a high He pressure for a few hours in a bombing chamber and subsequent transfer to a He spectrometer for He leak rate measurement.

Fine helium leak rate testing is considered to be one of the best means to characterize hermeticity quantitatively. However, this technique also has some limitations. In the leak rate tests, the sample has to be taken out of the He overpressure chamber and transferred to the He detector chamber. The leakage of helium during this transfer time cannot be accounted for.<sup>19</sup> It has been ensured that the transfer time is kept minimal. Ten samples were used for each bonding/aging condition in order to confirm the consistency.

There was a good correlation between the C-SAM analysis, microstructure characterization, shear strength measurements, and hermeticity testing. The hermeticity testing results of dies with isolated Au metallization and In interlayer (Fig. 1a) prior to bonding are listed in Table III. All the dies without

**Table III. Comparison of helium leak rate testing results with and without diffusion barriers**

S. no.	Without diffusion barriers		With diffusion barriers		
	Without Au protective coverage layer (atm cc/s)	With Au protective coverage layer (atm cc/s)	Ti (atm cc/s)	Pt (atm cc/s)	Ni (atm cc/s)
1.	$0.2 \times 10^{-5}$	$0.1 \times 10^{-7}$	$0.2 \times 10^{-7}$	$4.8 \times 10^{-7}$	$0.5 \times 10^{-7}$
2.	$1.3 \times 10^{-5}$	$0.2 \times 10^{-8}$	$1.3 \times 10^{-6}$	$0.2 \times 10^{-8}$	$0.3 \times 10^{-8}$
3.	$0.8 \times 10^{-6}$	$0.5 \times 10^{-8}$	$1.0 \times 10^{-5}$	$2.5 \times 10^{-7}$	$0.3 \times 10^{-8}$
4.	$0.4 \times 10^{-7}$	$2.2 \times 10^{-6}$	$1.0 \times 10^{-5}$	$1.6 \times 10^{-7}$	$0.6 \times 10^{-8}$
5.	$0.2 \times 10^{-6}$	$0.7 \times 10^{-8}$	$0.2 \times 10^{-7}$	$3.2 \times 10^{-7}$	$5.5 \times 10^{-7}$

**Table IV. Impact of thermal aging at 300 °C for 500 h on hermeticity**

S. no.	Ti diffusion barrier (atm cc/s)	Pt diffusion barrier (atm cc/s)	Ni diffusion barrier (atm cc/s)
1.	$1.9 \times 10^{-6}$	$4.8 \times 10^{-7}$	$2.1 \times 10^{-7}$
2.	$0.8 \times 10^{-5}$	$0.2 \times 10^{-8}$	$1.5 \times 10^{-7}$
3.	$2.6 \times 10^{-7}$	$5.5 \times 10^{-7}$	$4.4 \times 10^{-8}$
4.	$0.7 \times 10^{-5}$	$1.6 \times 10^{-8}$	$1.6 \times 10^{-9}$
5.	$0.5 \times 10^{-7}$	$0.7 \times 10^{-7}$	$5.5 \times 10^{-8}$

the Au protective coverage layer did not comply with the specification defined by the Military Standard test MIL-STD-883 for hermeticity. Close to half the number of dies with a thin Au protective layer over the In interlayer (Fig. 1b) met the military specification. The improvement in hermeticity for dies with the thin Au protective layer could be attributed to the fact that the formation of indium oxide, which hampers the TLP bonding process, is averted.

The hermeticity testing results of Au/In multi-stacked dies involving different diffusion barriers are listed in Table III. None of the dies involving a Ti diffusion barrier complied with the military specification. Few dies using a Pt diffusion barrier met the requirement. Close to half the number of dies involving a Ni diffusion barrier exceeded the target. This could be attributed to the fact that Ni serves as a better high-temperature diffusion barrier for the mentioned reasons.

It has been determined that the thermal aging significantly improves the hermeticity of Au/In multi-stacked dies. The hermeticity testing results of Au/In multi-stacked dies involving different diffusion barriers for samples aged at 300 °C for 500 h are listed in Table IV. No improvement in hermeticity was observed for the Ti diffusion barrier. Few dies involving the Pt diffusion barrier complied with the military specification. Many dies involving the Ni diffusion barrier exceeded the requirement. Improvement in hermeticity for dies involving a Pt and Ni diffusion barrier during thermal aging at 300 °C for various durations was observed. This

could be attributed to the growth of IMCs during thermal aging. In this context, the enhancement of hermeticity is linked to the kinetics of IMCs growth. Furthermore, the reduction of micro-cracks resulting in the bond quality improvement, as confirmed by SEM cross-section, also has a dramatic impact on the hermeticity.

The highest percentage of dies that could comply with the military specification was achieved for Au/In multi-stacked wafers involving the Ni diffusion barrier. Although dramatic improvement was observed, when subjected to thermal aging at 300 °C, 100 % yield could not be achieved. Few dies in an eight-inch wafer involving similar stacking, bonding, and aging conditions could meet the stringent Military Standard requirement. Thus, hermetic WLB for such fast reactive metallic systems requiring very low activation energy for diffusion even at room temperature is yet to be fully resolved.

## CONCLUDING REMARKS

It was determined that the temperature ramp rate has a direct impact on the Au-In bond quality. Very high ramp rates are required to avert the transformation of the low-melting interlayer such as In into IMCs prior to bonding. Wafer-level hermetic sealing could be achieved for multi-stacked Au-In wafers only by using a thin film diffusion barrier. Prospective diffusion barriers could alter the isothermal solidification during TLP bonding. Among the diffusion barriers investigated, Ni was determined to be the most appropriate. This could

be attributed to the presence of  $\alpha_1$  phase at the interface, since the interdiffusion of Au and In in this phase is relatively lower. The AuIn and AuIn<sub>2</sub> IMCs were determined to be thermally stable at 300 °C for 500 h. No degradation in the shear strength was observed when subjected to thermal aging and thermal cycling conditions. Hence, it was concluded that Au-In is a prospective candidate for hermetic sealing of MEMS sensors for down-hole application. Moreover, improvement in hermeticity was confirmed when subjected to thermal aging at 300 °C due to the reduction in voids/micro-cracks at the interface.

### ACKNOWLEDGEMENT

The authors acknowledge the Singapore Science and Research Council (SERC—Grant No. 102 165 0082) for financial support through the innovation consortium “Rugged Electronics” program.

### REFERENCES

1. J. Watson, High-temperature electronics pose design and reliability challenges (Analog Dialogue, April 2012), <http://www.analog.com/library/analogDialogue/>. Accessed 15 July 2013.
2. V. Chidambaram, H.B. Yeung, and G. Shan, *J. Electron. Mater.* 41, 8 (2012).
3. S.-H. Choa, *J. Microsyst. Technol.* (2005). doi:10.1007/s00542-005-0603-8.
4. W.C. Welch III and K. Najafi, *Proceedings of the International Conference on MEMS* (Tucson, United States, 2008), p. 806.
5. W. Zhang, A. Matin, E. Beyne, and W. Ruythooren, *Proceedings of the Electronic Components and Technology Conference* (Singapore, 2008), p. 1984.
6. H. Okamoto, *Binary Alloy Phase Diagrams*, updating service (ASM International Materials Park, 1992).
7. F.S. Shieu, C.F. Chen, J.G. Sheen, and Z.C. Chang, *Thin Solid Films* 346, 1 (1999).
8. J. Baborowski, A. Pezous, G.S. Durante, R.J. James, R. Ziltener, C. Muller, and M.-A. Dubois, *Proceedings of the Euroensors XXIII Conference* (Lausanne, Switzerland, 2009), p. 1535.
9. S.T. Riches, C. Johnston, M. Sousa, P. Grant, J. Guilliver, M. Langley, R. Pittson, and M. Firmstone, *Proceedings of the International Conference of High-Temperature Electronics* (Albuquerque, United States, 2008), p. 265.
10. C. Johnston, *Proceedings of the International Conference of High-Temperature Electronics* (Albuquerque, United States, 2008), p. 1.
11. W. Zhang and W. Ruythooren, *J. Electron. Mater.* 37, 8 (2008).
12. J. Bjontegaard, L. Buene, T. Finstad, O. Lonsjo, and T. Olsen, *Thin Solid Films* 101, 253 (1983).
13. W. Zhang, A. Matin, E. Beyne, and W. Ruythooren, *Proceedings of the Electronic Components and Technology Conference* (Singapore, 2008), 1984.
14. X.-N. Xu, Y.-P. Ren, C.-F. Li, L. Song, and G.-W. Qin, *Trans. Nonferrous Met. Soc. China* 22, 6 (2012).
15. A.N. Torgensen, L. Offernes, A. Kjekshus, and A. Olsen, *J. Alloy. Compd.* 314, 1–2 (2001).
16. M. Waelti, N. Scheeberger, O. Brand, and H. Baltes, *Proceedings of the International Symposium on Materials Research Society* (San Francisco, United States, 2000), p. 183.
17. X.J. Huang, S.-W. Ricky Lee, and W.S. Tae, *Proceedings of the Electronic Components and Technology Conference* (Singapore, 2000), p. 86.
18. S. Egelkraut, L. Frey, M. Knoerr, and A. Schletz, *Proceedings of the 12th Electronic Packaging Technology Conference* (Singapore, 2010), p. 660.
19. I. De Wolf, A. Jourdain, P. De Moor, A.C. Tilmans, and L. Marchand, *Proceedings of the International Symposium on the Physical and Failure Analysis of Integrated Circuits* (Bangalore, India, 2007), p. 147.